Physics – Uspekhi **51** (5) 427 – 435 (2008)

REVIEWS OF TOPICAL PROBLEMS PACS numbers: **36.40.–c**, **74.70.–b**, 74.78.Na

'Giant' strengthening of superconducting pairing in metallic nanoclusters: large enhancement of T_c and potential for room-temperature superconductivity

V Z Kresin, Yu N Ovchinnikov

DOI: 10.1070/PU2008v051n05ABEH006531

Contents

Abstract. In relation to the recently intensified search for new superconducting systems, it is interesting to study the properties of metal nanoclusters containing $\sim 10^2 - 10^3$ free carriers. It is essential that the spectra of delocalized electrons in many clusters form energy shells similar to those in atoms and nuclei. The superconducting pairing can be very strong if the cluster parameters satisfy certain conditions. Such clusters constitute a new family of high-temperature superconductors (with $T_c \geqslant 150$ K). Transition into the superconducting state is manifested in an essential rearrangement of the energy spectrum. Pair correlation affects the optical, magnetic, and thermodynamic properties of clusters; corresponding changes can be detected in specific experiments. Clusters can form high-temperature superconducting tunneling networks, and this leads to macroscopic high-temperature superconductivity. In principle, higher values of T_c, up to room temperature, may be achieved.

V Z Kresin Lawrence Berkeley Laboratory,
University of California Berkeley, CA 94720, USA
Tel. 1 (510) 48 69 91. Fax 1 (510) 482 25 30
E-mail: vzkresin@lbl.gov
Yu N Ovchinnikov Landau Institute for Theoretical Physics,
Russian Academy of Sciences,
ul. Kosygina 2, 117334 Moscow, Russian Federation,
Tel. (7-495) 702 93 17. Fax (7-495) 938 20 77
E-mail: ovc@itp.ac.ru
Max-Planck Institute for the Physics of Complex Systems,
Dresden, D-01187, Germany

Received 5 December 2007
Uspekhi Fizicheskikh Nauk **178** (5) 449 – 458 (2008)
DOI: 10.3367/UFNr.0178.200805a.0449
Translated by V V Losyakov; edited by A M Semikhatov

1. Introduction

This paper is concerned with the superconducting state in small metallic nanoclusters. It can be demonstrated [1 – 3] that nanoclusters form a new family of high-temperature superconductors.

The study of the superconducting state in nanoparticles is not a new field (see, e.g., reviews [4, 5]). Moreover, the study of granular superconductors has a long history (see, e.g., [6 – 8]) and directly touches upon the question of pairing in separate granules. The most recent and advanced study of nanoparticles was performed by M Tinkham and his group [9 – 11]. Particles were placed inside a tunneling barrier, and special features of their electronic spectra, including the odd – even effect, were detected. The nanoparticles studied in [9 – 11] were relatively large, with the size $d \sim 50 - 100$ Å, and therefore they contain $\sim 10^4 - 10^5$ electrons. Here, we focus on much smaller nanoclusters containing $\sim 10^2$ delocalized electrons.

The study of nanoclusters has attracted much attention since the discovery of a shell structure in their electronic spectra [12]. We discuss this fundamental feature in Section 2. It is essential to stress that precisely because of the shell structure, high values of the critical temperature may be expected for some selected clusters. Potentially, the values of T_c can reach room temperature.

The structure of this paper is as follows. Shell structure is described in Section 2. Section 3 contains a qualitative description of pairing in nanoclusters and the role of shell structure. The qualitative reason for expecting high T_c values is presented. The main equations and the method for calculating T_c are introduced in Section 4, and some specific examples are considered. Section 5 contains an analysis of the energy spectrum (energy gap) near $T = 0$ K. A Ginzburg –

Landau functional that allows studying various properties near T_c can also be introduced: the role of fluctuations is discussed. Section 6 is concerned with various manifestations of the pair correlation and the possibility of their experimental observation. The properties of nanocluster-based tunneling networks capable of transmitting a macroscopic superconducting current are described in Section 7. Section 8 contains concluding remarks.

2. Metallic nanoclusters. Energy shells

Clusters are the aggregates of atoms (or molecules) that have the structure A_k, where k is the number of atoms A (e.g., Na_k, Ga_k). The number k of atoms can vary from 2 to any large value, and therefore the study of clusters allows tracking the evolution from isolated atoms to solids. Metallic clusters, like any metallic systems, are characterized by the presence of delocalized electrons; their subsystem is formed by the valence electrons of the atoms. The number N of valence electrons is the main parameter of the cluster. For simple monovalent metallic clusters, such as Na_k and Li_k, we have $N = k$. For more complicated clusters, $N = vk$, where v is the number of valence electrons per atom, for example, $N = 135$ for Al_{45} clusters, because each Al atom contains 3 valence electrons. With the use of mass spectroscopy, the specific clusters can be selected. We also note that because of the finite size, the electronic energy spectrum of an isolated cluster is discrete.

Clusters are usually prepared by evaporation of metals, and hence their initial temperature is rather high. There are various experimental techniques for cooling the clusters. As a result, cluster beams at different temperatures can be produced.

A milestone discovery was made in 1984 when W Knight and his collaborators discovered [12] that the electronic spectra in many metallic clusters form energy shells similar to those in atoms or atomic nuclei. The shell structure is a key feature of nanoclusters (see reviews [13–16]). As is known, the atoms with complete shells (s, d, ..., f-shells) are the most stable. The same is true for nucleons in atomic nuclei (see, e.g., [17]). Specific clusters that are most stable can be distinguished (Fig. 1). Similarly to inert atoms, energy shells for such clusters are completely occupied; such clusters are called 'magic.' Some examples of such close-shell clusters are $N_m = 8, 20, 40, 58, 92, 132, 138$.

It is essential that the 'magic' clusters with a good accuracy have the spherical symmetry. As a result, their electronic states can be classified by the orbital momentum L and radial quantum number n. If the energy shell is incomplete, the cluster undergoes a Jahn–Teller distortion and its shape deviates from spherical (Fig. 2). As a result, the energy level with a specific value of L splits, and hence the electronic states of the deformed cluster can be classified not by L but by a projection of the angular momentum m. The scale of the shell splitting is different for different metals and also depends on the number of delocalized electrons, more specifically, on the deviation δN from the nearest 'magic' number ($\delta N = N - N_m$). In turn, the change in shape affects the electronic energy spectrum. An interesting and unique correlation between the number of electrons and the energy spectrum can therefore be observed; this is a remarkable feature of metallic clusters.

Shell structure was discovered initially for simple monovalent alkali clusters, such as sodium (Na) and potassium (K). Later, this phenomenon was also observed for Al, Ga, In, Zn, and Cd clusters (see, e.g., [18–21]). It is interesting that energy shells are not a universal feature. For example, for Nb clusters, the spectrum does not display a shell structure.

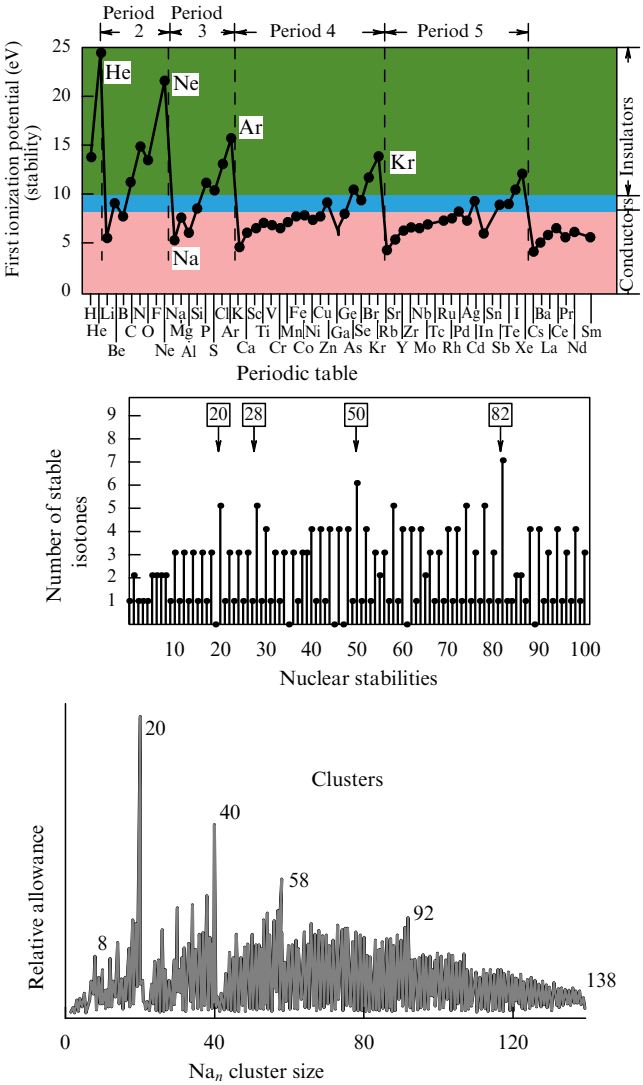

Figure 1. Shell structures for atoms, nuclei, and nanoclusters; 'magic' numbers.

As electrons are added to the lowest unoccupied shell (LUS), the shape deforms from spherical and becomes prolate. In this case, the energy levels are four-degenerate: $(m, -m)$ and $(s_z, -s_z)$. The residual orbital degeneracy is removed [22] by oscillations (the dynamic Jahn–Teller effect) between two configurations similar to Kekule structures of benzene molecules (see, e.g., [23]). But this question is beyond the scope of this paper.

Energy levels in magic clusters are totally occupied up to the highest occupied shell (HOS). This shell and the LUS play a major role in our analysis. They are analogous to the HOMO and LUMO orbitals in molecular spectroscopy. As was mentioned above, clusters with an incomplete HOS undergo a Jahn–Teller deformation. As a result, all shells, including HOS and LUS, are split and form manifolds; each sublevel of such a manifold is characterized by $|m|$, where m is the angular momentum projection.

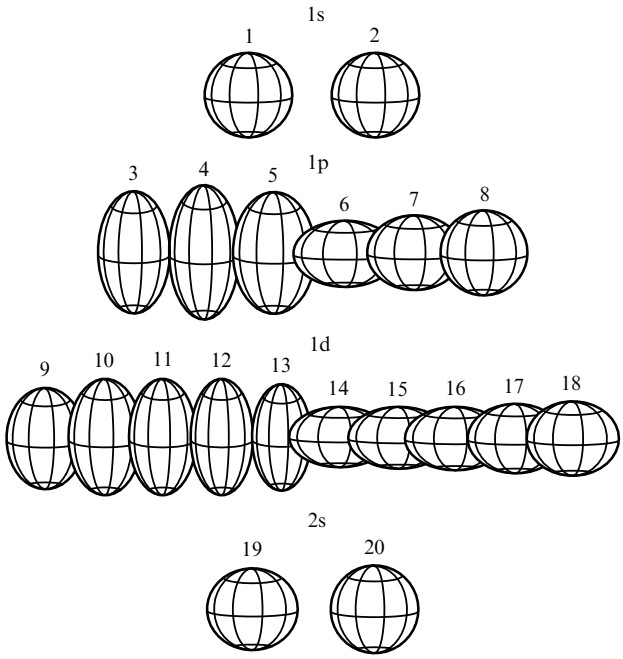

Figure 2. Cluster shapes for various values of N.

3. Superconducting state and high T_c. Qualitative picture

As we know, the Cooper pairs in bulk superconductors are formed by electrons with opposite momenta and spins. For the nanoclusters of interest, the momentum is not a quantum number, and the pairs are formed by electrons with opposite projections of the angular momentum $(m, -m)$. In many aspects, the picture of pairing is similar to that in atomic nuclei (see, e.g., [24–26] and review [17]). In each case (nucleus or cluster), we are dealing with a finite Fermi system and a shell structure. The pairing states are labeled by similar quantum numbers $(m, -m)$. The manifestation of pairing has similar features (see below). However, we can develop a microscopic approach for clusters because we know the forces (Coulomb interaction). In addition, the presence of two subsystems (electrons and ions) allows using the adiabatic Born–Oppenheimer approximation.

We focus on the HOS. For 'magic' clusters, the states are degenerate, and the degree of degeneracy $2(2L+1)$ depends on the value of the orbital momentum. For clusters with an incomplete shell, the states with different values of $|m|$ (where m is the projection of orbital momentum) correspond to different energy levels, and the corresponding summation must be performed (see below, Section 3).

As mentioned above, the pairing occurs between the states $(m, -m)$. The pair correlation strength varies for different clusters. Correspondingly, the critical temperature T_c and the energy gap strongly depend on the cluster parameters, its shape, the coupling strength, etc. We consider specific cases below.

It is important that under special but perfectly realistic conditions, high values of T_c can be observed. Qualitatively, this can be understood as follows. We consider the case where the highest occupied shell is highly degenerate ($2(2L+1)$ is large). This can be viewed as a sharp peak in the density of states at the Fermi level. The situation is similar to that studied in [27] for bulk materials; the presence of a peak in the density of states (van Hove singularity) results in a noticeable increase in T_c. It is essential that the density of states in the clusters of interest is strongly peaked at the Fermi level.

We discuss one more point. The most distinguished feature of small nanoparticles is the discrete nature of the electronic spectrum. As was noticed in [5, 28], the superconducting state can manifest itself if the pairing energy gap Δ exceeds or is comparable to the energy spacing caused by the finite size of the particle, that is, if $\Delta \gtrsim \Delta E$, where, $\Delta E = E_F/N$ is the average energy level spacing and Δ is the energy gap. According to the estimation in [28], $E_F \approx 10^5$ K and $\Delta \approx 10$ K, and therefore N should be relatively large: $N \gtrsim 10^4$. As a result, if we are concerned with small nanoclusters, $N \approx 10^2 - 10^3$, it might seem that they do not display superconducting properties, because the average level spacing ($E_F/N \sim 10^2 - 10^3$ K) greatly exceeds the pairing energy gap. But such an estimation can be challenged. Indeed, for larger T_c (e.g., $T_c \approx 40$ K for MgB_2 and $T_c \approx 10^2$ K for cuprates; for nanoclusters, T_c can be even higher: see below), the energy gap is much larger than 10 K, and this leads to a noticeable decrease in the limiting value of N. More importantly, the estimation is based on the assumption that the energy levels are approximately equidistant. The discovery of shell structure totally invalidates this assumption; the real situation is more complex. It turns out that for many real clusters, the pattern of electronic states is very different from an equally spaced level distribution. Instead, they contain highly degenerate energy levels, or groups of very close levels, such that the energy spacing for electronic states close to the Fermi level E_F appears to be rather small (Fig. 3). The situation in such clusters is very favorable for pairing. Moreover, we can even expect a giant strengthening of the phenomenon relative to bulk samples (see below).

The importance of shell structure for pairing was stressed by W Knight [29] (see also [30, 31]). Especially interesting was the paper by J Friedel [32], who was motivated by the discovery of C_{60} clusters and superconductivity in fullerides. According to [32], if clusters with a half-filled shell have a spherical shape, they would have high values of T_c. However, for such a shell filling, the cluster Jahn–Teller deformation would be very large, drastically decreasing T_c. In connection with this, the use of cluster networks was suggested in [32], with the resulting charge transfer leading to a resolution of this problem. The idea of such a superconducting molecular crystal (or, more precisely, cluster crystal) is very interesting.

As noted above, shell structure was discovered in 1984. It took several more years for this concept to become generally accepted (see, e.g., review [13]). But by the early 1990s, the superconducting community was preoccupied with the new family of high-T_c cuprates [33, 34]. Nevertheless, the discovery in [12] was followed by several interesting papers

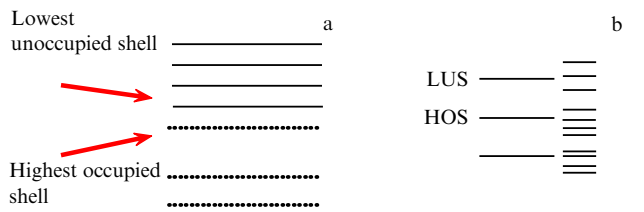

Figure 3. Energy spectra for a 'magic' cluster (a) and in the case of a nearly complete shell (b).

discussing pairing in clusters. It can be hoped that the experimental study of the superconducting state of nanoclusters with its potential for room-temperature superconductivity (see Section 4) will attract the attention it deserves.

We first discuss pairing in isolated clusters. The tunneling network is described below (Section 7).

4. Critical temperature

The equation for the pairing order parameter $\Delta(\omega_n)$ has the form

$$\Delta(\omega_n)\, Z = \eta\, \frac{T}{2V} \sum_{\omega_{n'}} \sum_s D(\omega_n - \omega_{n'})\, F_s^+(\omega_{n'})\,, \tag{1}$$

where $\omega_n = (2n+1)\,\pi T$, $n = 0, \pm 1, \pm 2, \ldots$ (we use the thermodynamic Green's function formalism, see, e.g., [35]),

$$D(\omega_n - \omega_{n'}, \widetilde{\Omega}) = \widetilde{\Omega}^2 \left[(\omega_n - \omega_{n'})^2 + \widetilde{\Omega}^2\right]^{-1} \tag{1'}$$

is the vibrational propagator,

$$F_s^+(\omega_{n'}) = \Delta(\omega_{n'}) \left[\omega_{n'}^2 + \xi_s^2 + \Delta^2(\omega_{n'})\right]^{-1} \tag{1''}$$

is the pairing function introduced by Gor'kov [36], $\xi_s = E_s - \mu$ is the energy of the sth electronic state referenced to the chemical potential μ, V is the cluster volume, $\eta = \langle I^2 \rangle / M\widetilde{\Omega}^2$ is the Hopfield parameter, $\langle I \rangle$ is the electron–ion matrix element averaged over electronic states involved in the pairing (see, e.g., [37, 38]), M is the ion mass, and Z is the renormalization function; we do not write the equation for Z here. We note that the presence of the renormalization function Z removes the divergence at $\omega_n = \omega_m$ [39]. The Coulomb term μ^* can be included in the usual way.

It can be seen from Eqn (1) that the electron–vibrational interaction is the mechanism of pairing. As we know, the BCS formalism is valid in the weak-coupling approximation (then $T_c \ll \widetilde{\Omega}$, where $\widetilde{\Omega}$ is the characteristic vibrational frequency). Because we want to go beyond this limit, we start with general equation (1), which explicitly contains the vibrational propagator. We note that in the weak-coupling case ($\eta/V \ll 1$ and, correspondingly, $\pi T_c \ll \widetilde{\Omega}$), $Z = 1$ and $D = 1$ must be set in Eqn (1), recovering the usual BCS scheme for the bulk sample.

Equation (1) contains a summation over all discrete electron states. For 'magic' clusters that have a spherical shape, we can replace summation over states by summation over the shells: $\sum_s \to \sum_j G_j$, where $G_j = 2(2I_j + 1)$ is the shell degeneracy and I_j is the orbital momentum. If the shell is incomplete, the cluster undergoes a Jahn–Teller deformation; as a result, its shape becomes ellipsoidal and the states s are classified by the projection of orbital momentum $|m| \leqslant I$, with each level containing up to four electrons (for $|m| \geqslant 1$).

Equation (1) looks similar to that in the theory of strong-coupling superconductivity [40], but is different in two key aspects. First, it contains a summation over discrete energy levels E_s, whereas for a bulk superconductor, integration over the continuous energy spectrum (over ξ) is performed. Another important difference is that in contrast to a bulk superconductor, here we are dealing with a finite Fermi system, and therefore the number N of electrons is fixed. As a result, the position of the chemical potential differs from the Fermi level E_F and is determined by the values of N and T. Specifically, we can write

$$N = \sum_n \sum_s \mathfrak{I}_s(\omega_n)\, \exp\left(\mathrm{i}\omega_n \tau\right)_{\tau \to 0} = \sum_s \left(u_s^2 \varphi_s^- + v_s^2 \varphi_s^+\right), \tag{2}$$

where $\mathfrak{I}_s(\omega_n)$ is the thermodynamic Green's function,

$$u_s^2, v_s^2 = 0.5\left(1 \mp \frac{\xi_s}{\varepsilon_s}\right), \quad \varphi_s^{\mp} = \left[1 + \exp\left(\mp \frac{\varepsilon_s}{T}\right)\right]^{-1}, \tag{3}$$

$$\varepsilon_s = \left(\xi_s^2 + \varepsilon_{0,s}^2\right)^{1/2}, \tag{4}$$

$\varepsilon_{0,s}$ is the gap parameter for the sth level, and $\varepsilon_{0,s}$ is the root of the equation $\varepsilon_{0,s} = \Delta(\mathrm{i}\varepsilon_{0,s})$. Because $\xi_s = E_s - \mu$, Eqn (2) determines the position of the chemical potential for the given number N of electrons, as well as the dependence $\mu(T)$.

Equations (1) and (2) and the equation for the renormalization function Z form the system of equations describing the superconducting state of metallic nanoclusters.

We also note that for the clusters of interest ($N \geqslant 10^2$; then $k_H R \gg 1$), the order parameter $\Delta \equiv \Delta(\omega_n)$; the coordinate dependence and, consequently, the dependence on s is rather weak (see, e.g., [41]) and can be neglected. Here, R is the cluster radius and k_H is the electron wave vector for the highest occupied shell ($k_H \approx 2/r_s$, where r_s is the electron density parameter; we set $\hbar = 1$). The value of k_H for the clusters of interest is close to the Thomas–Fermi screening wave vector and to the Fermi momentum k_F. The energy E_H of the HOS is likewise close to the bulk Fermi energy E_F.

We make one more general remark. The theory of usual bulk superconductors encounters a strong logarithmic singularity (Cooper instability, see, e.g, [35]). The situation for nanoparticles is different. Because of the discrete energy spectrum, we are dealing with a threshold phenomenon, and hence even at low T_c, the value of the coupling constant must exceed some critical value. However, we focus on the opposite case in what follows, with large values of T_c.

At $T = T_c$, we should set $\Delta = 0$ in the denominator of expression (1″), which yields

$$\Delta(\omega_n)\, Z = \eta\, \frac{T}{2V} \sum_{n'} \sum_s \frac{\widetilde{\Omega}^2}{\widetilde{\Omega}^2 + (\omega_n - \omega_{n'})^2}\, \frac{\Delta(\omega_{n'})}{\omega_{n'}^2 + \xi_s^2}\,. \tag{5}$$

The value of the parameter η is close to its bulk value η_b. Indeed, the surface of the cluster can be treated as a scatterer (cf. [42]), and therefore the pairing is analogous to that in the case of a 'dirty' superconductor (see, e.g., [43]), where the mean free path is much shorter than the coherence length. Then the average value of I^2 is not affected by the scattering and it indeed follows that $\eta \approx \eta_b$, where η_b is the bulk Hopfield parameter (see, e.g., [38]). We also note that the characteristic vibrational frequency is close to the bulk value because pairing is mediated mainly by the short-wavelength part of the vibrational spectrum. Then Eqn (5) can be written as

$$\Delta(\omega_n)\, Z = \lambda_b\, \frac{T}{2\nu_b V} \sum_{n'} \sum_s \frac{\widetilde{\Omega}^2}{\widetilde{\Omega}^2 + (\omega_n - \omega_{n'})^2}\, \frac{\Delta(\omega_{n'})}{\omega_{n'}^2 + \xi_s^2}\bigg|_{T_c}, \tag{6}$$

where $\lambda_b = \eta \nu_b$ is the bulk coupling constant [44] and $\nu_b = m^* p_F / 2\pi^2$ is the bulk density of states.

We consider the strong-coupling case ($2\pi T_c/\widetilde{\Omega} \gtrsim 1$). Then it is convenient to use the matrix method [45–47]. This method was used in our paper [3]. The critical temperature can be obtained from the matrix equation

$$\det |1 - K_{nn'}| = 0\,, \quad n, n' \geqslant 0\,. \tag{7}$$

For 'magic' clusters, the kernel has the form

$$K^c_{nn'} = g\tau_c \sum_j G_j (f^-_{n;n'} + f^+_{n;n'+1})\, \chi_{n';\tilde{\xi}}\,, \quad n \neq n'\,,$$

$$K^c_{nn} = g\tau_c \sum_j G_j \Big\{ \frac{1}{2}\, \chi_{n;0.5}\, \chi_{n;\tilde{\xi}_j} - \left(n + \frac{1}{2}\right)^{-1} \times$$

$$\times \tau_c^2 \sum_{m \neq n} \left[(m+n+1)^2 - (n-m)^2\right] f^-_{n;m}\, f^+_{n;m+1} \left(m + \frac{1}{2}\right) \chi_{m;\tilde{\xi}_j} \Big\}. \tag{8}$$

where $\tilde{\xi} = \xi/\widetilde{\Omega}$ and

$$f^{\pm}_{n;r} = \left[1 + (n \pm r)^2 \tau_c^2\right]^{-1}, \tag{8'}$$

$$\chi_{n;\tilde{\xi}} = \left[\left(n + \frac{1}{2}\right)^2 \tau_c^2 + \tilde{\xi}^2\right]^{-1}. \tag{8''}$$

As noted above, we focus on the case where $\tau_c = 2\pi T_c/\widetilde{\Omega} \gtrsim 1$. In this case, matrix equation (7) converges rapidly. The main contribution to the sums over shells in Eqn (8) usually comes from the highest occupied shell and the lowest unoccupied shell, and hence, with sufficient accuracy, we can consider two terms ($j = \mathrm{H}, \mathrm{L}$ with $G_H = 2(2I_H + 1)$ and $G_L = 2(2I_L + 1)$, where I_H and I_L are the corresponding angular momenta). To estimate the value of T_c, we can use the equation $1 - K_{00} = 0$, which can be reduced to the simple form

$$1 = g_{\mathrm{eff}} F(\tau_c; \Delta\widetilde{E})\,,$$
$$g_{\mathrm{eff}} = 8g(G_H + G_L)\,, \tag{9}$$

where $g = \lambda_b (4\pi\widetilde{\Omega}\nu_b V)^{-1}$, $\tau_c = 2\pi T_c/\widetilde{\Omega}$, $\Delta E = E_L - E_H$ is the spacing between the highest occupied and the lowest unoccupied shells, and

$$F(\tau_c; \Delta\widetilde{E}) = \tau_c(\tau_c^2 + 1)^{-1} \Big\{ \left[\tau_c^2 + (\Delta\widetilde{E})^2\right]^{-1}$$
$$- 4.5\tau_c^2 \left[(4\tau_c^2 + 1)^{-1} \left(9\tau_c^2 + (\Delta\widetilde{E})^2\right)\right]^{-1} \Big\}.$$

It follows directly from Eqn (9) that the high degeneracies of the HOS and the LUS play a very important role. Qualitatively, these degeneracies increase the effective electron–vibration coupling g_{eff}, and, more specifically, the effective density of states. It is essential that the value of T_c depends on the parameters that can be obtained from experimental measurements (ΔE, $\widetilde{\Omega}$, λ_b, ν_b) or from symmetry considerations (degeneracies G_H and G_L; see, e.g., Ref. [48]). Photoemission or ionization potential measurements appear to be the best techniques to determine the electron energy spectrum.

We first demonstrate that for perfectly realistic values of the parameters, a high value of T_c can be obtained. We consider the following set of parameters: $\Delta E = 0.065$ eV, $\widetilde{\Omega} = 25$ meV, $m^* = 0.75 m_e$, $k_F = 1.5 \times 10^8$ cm^{-1}, $\lambda_b = 0.5$, the radius $R = 6$ Å, and $G_H + G_L = 48$ (e.g., $I_H = 7$, $I_L = 4$, and $N = 168$); then $g \approx 0.2$. With Eqns (7) and (8), we obtain $T_c = 160$ K (!).

The value of T_c is very sensitive to the cluster parameters. The most favorable case corresponds to

1) a cluster with large values of the orbital momentum L for the highest occupied and lowest unoccupied shells, and hence with large degeneracies G_H and G_L, and

2) a relatively small energy spacing between these shells.

For example, clusters with $N = 168$ (e.g., Ga_{56} or Zn_{83}) satisfy these criteria. We also note that the situation becomes less favorable for large clusters because the shell effect then weakens and, in addition, the decrease in the energy level spacing leads to a broad distribution of the density of states and to the loss of its peak structure.

Of course, the cluster should display the presence of the shell structure for the T_c value to be high. For example, according to [49], Nb clusters undergo the transition to the superconducting state. But the value of T_c is not increased relative to its bulk value, which is due to the absence of shells for Nb clusters.

Our paper [3] contains calculations for specific clusters. For example, we consider the Ga_{56} cluster. It contains $N = 168$ delocalized electrons. Using the values $\lambda_b = 0.4$, $\Delta E \approx 0.1$ eV, $\widetilde{\Omega} = 270$ K, $G_H + G_L = 60$, $m \approx 0.6 m_e$, and $R \approx 6.5$ Å and estimating T_c from Eqn (9), we obtain $T_c \approx 170$ K. A more accurate calculation based on Eqns (7) and (8) leads to $T_c \approx 145$ K, which greatly exceeds the bulk value $T_c^b \approx 1.1$ K. Similarly, we obtained $T_c \approx 105$ K for Zn_{190}.

An increase in T_c can be achieved by changing the parameters (ΔE, $\widetilde{\Omega}$, etc.) in the desired direction. For example, for $\Delta E \approx 0.2$ eV, $\lambda_b \approx 0.5$, $m \approx 0.5 m_e$, $R \approx 5.5$ Å, $\widetilde{\Omega} = 50$ meV, and $G_H + G_L = 60$, we obtain $T_c \approx 240$ K (!). In principle, T_c can be increased to room temperatures.

The analysis can be generalized for clusters with nearly complete shells (e.g., $N = N_m - 2$, N_m). The density of states is now spread over different energy levels, and such weakening of the sharp peak feature is not a positive factor for T_c. On the other hand, the removal of electrons from the HOS strongly affects the position of the chemical potential, and this factor turns out to be favorable for pairing. The best scenario would correspond to clusters with almost filled shells (e.g., $N = N_m - 2$ being a 'magic' number) and, correspondingly, a small deviation from the spherical shape. In this case, the HOS turns into a set of close levels classified by $|m|$, where m is the projection of the angular momentum. High values of T_c can be expected for such clusters [3].

5. Energy gap. The Ginzburg–Landau functional

Pairing leads to a noticeable modification of the cluster electron spectrum. The energy gap opens at $T < T_c$ and its opening greatly affects the energy spectrum: the spacing between HOS and LUS becomes different. We can study its behavior near $T = 0$ and near T_c [3]. The energy gap at $T = 0$ K can be calculated from Eqn (1) written at $T = 0$ (then the summation over ω_n can be replaced by integration). The energy gap $\varepsilon_{0,s}$ near the level $\xi_s = E_s - \mu$ can be determined from the equation $\varepsilon_{0,s} = \Delta\left[\mathrm{i}(\xi_s^2 + \varepsilon_{0,s}^2)^{1/2}\right]$. For example, for a cluster with the realistic set of parameters $\Delta E = 65$ meV, $E_F = 8$ eV, $\widetilde{\Omega} = 24$ meV, and $\lambda_b = 0.4$, we obtain the HOS–LUS spacing $\Delta\varepsilon = 80$ meV. This value

noticeably exceeds the intershell spacing in the absence of pairing, $\Delta E = 65$ meV. An especially large effect can be observed for clusters with nearly complete shells, when the energy gap parameter is comparable with the shell splitting caused by the JT effect.

As we know, there is no phase transition for infinite 1D and 2D systems, and this is due to fluctuations. It might be thought that nanoclusters should be treated as 0D systems and that the impact of fluctuations is the critical factor destroying the superconducting state. But the situation is not so simple. Indeed, the dimensionality of a system is determined by the relation between its size and some characteristic scale. For the superconducting state, the coherence length represents such a scale. For example, a thin film is considered a 2D system because its thickness is small relative to the coherence length. But the value of the coherence length is not universal and varies greatly for different systems. For example, for conventional superconductors, the coherence length is large, being of the order of $5 \times 10^2 - 10^3$ nm. However, the situation is different for cuprates: the high value of the critical temperature leads to a relatively small coherence length (~ 15 Å).

For nanoclusters, we should also compare the cluster size and the corresponding coherence length. For high-T_c nanoclusters, similarly to the cuprates, the coherence length appears to be short and is of the order of 10 – 15 Å. Therefore, it is comparable with the cluster size. As a result, clusters with high T_c represent 3D systems, and the phase transition is observable.

This is a rather qualitative argument. But the fluctuation problem can be studied in more detail. The Ginzburg – Landau functional can be derived as [3]

$$\delta\widetilde{\Theta}_s = \widetilde{A}\left[-(\tau_c - \tau)\, b^2 + (2\sigma)^{-1} b^4\right], \tag{10}$$

where $b^2 = \sigma\delta\tau$, $\delta\tau = \tau_c - \tau$, $\tau = 2\pi T/\widetilde{\Omega}$, and $\widetilde{A}$ and σ are constants defined in [3]. Based on Eqn (10), the broadening of the transition $\delta T_c/T_c$ due to fluctuations can be calculated.

A direct calculation performed for various specific clusters shows that the transition broadening is of the order of $\delta T_c/T_c \approx 5\%$. Such a broadening noticeably exceeds that for bulk superconductors ($\sim 10^{-8}$ K), but is still relatively small.

6. How to observe the phenomenon?

If it is possible to build a cluster-based tunneling network (see below, Section 7), that would allow transmitting a high-temperature macroscopic superconducting current. But we first focus on various manifestations of the pair correlation for an isolated cluster. We discuss the possibility of their experimental observation.

6.1 The energy spectrum and its temperature dependence

Pairing leads to a strong temperature dependence of the excitation spectrum. For $T > T_c$, the minimum excitation energy is given by $\Delta E_{\min} = E_L - E_H$ for magic clusters and by $\Delta E_{\min} = E^H_{|m|=I} - E^H_{|m|=I-1}$ for clusters with nearly complete shells. Below T_c and especially at low temperatures near $T = 0$, the excitation energy $\Delta E_{\min}(T = 0)$ is strongly modified by the gap parameter and noticeably exceeds the energy in the region $T > T_c$. The shift is especially dramatic for clusters with nearly occupied shells; the ratio $\Delta E_{\min}(T = 0)/\Delta E_{\min}(T > T_c)$ can then be $\sim 6-7$. An interesting case corresponds to the overlap of HOS and LUS manifolds. Such an overlap leads to even greater values of the ratio. A change of such magnitude in the excitation energy should be experimentally observable and would represent a strong manifestation of the pair correlation.

Generating beams of isolated metallic clusters at different temperatures in combination with mass selection would allow focusing on clusters of a specific size at various temperatures. A measurement of the energy spectrum, in particular, a determination of $\Delta E_{\min}(T = 0)$ and $\Delta E_{\min}(T > T_c)$ (for example, by photoelectron spectroscopy; see, e.g., [50] and review [51]), would reveal a strong temperature dependence of the spectrum. For example, in Ga clusters ($N = 168$, $T_c \approx 130$ K), a large difference in ΔE should be observed at the low-temperature region and above $T_c \approx 130$ K. Similarly, for Cd clusters with $N = 166$, a large difference should be observed between spectra at low temperatures and for $T > T_c = 85$ K. The use of Ga and Cd nanoclusters for such experiments looks reasonable because these materials are superconducting and, as mentioned above, the existence of an electron shell structure in their clusters has been confirmed experimentally. An experiment of this type would be both realistic and informative. If it is possible to place small nanoclusters into a tunneling barrier, then the spectrum can be determined with the use of inelastic tunneling spectroscopy similar to that employed in [9 – 11]. In this case, there will be no problems related to optical selection rules.

The pair correlation can also manifest itself in odd – even effects in cluster spectra. The presence of an unpaired electron must strongly affect the excitation spectrum. A similar effect has been observed for the nucleus and is a manifestation of pair correlation. Such an effect was also observed in [11], albeit for much larger particles ($N \approx 10^4 - 10^5$). It would be interesting to perform similar spectroscopy for small nanoclusters displaying a shell structure, such as Ga_{56} or Cd_{83} .

6.2 Heat capacity

An interesting calorimetric study of clusters was performed by M Jarrold and his collaborators [52]. They developed a special method that allows measuring the heat capacity of an *isolated* cluster. The measurements were performed using a multicollisional induced dissociative method. This method is described in [53].

The beam of cluster ions selected by mass spectroscopy undergoes a variable extension, and the desired temperature is thus set. These clusters are then focused into a special collision cell, where they are heated by collisions with an He buffer gas. As a result, some of the clusters dissociate; the modified mass distribution is analyzed by a second mass spectrometer. The number of clusters that undergo the dissociation depends on their internal energy and its closeness to the dissociation threshold. The number of dissociated clusters is directly related to the cluster internal energy. The change in the dissociation threshold with temperature provides a measure of the heat capacity.

The study in [52] shows that for selected clusters, e.g., for Al_{45} ions, a peak in heat capacity can be observed. It is essential that the peak is not a universal feature and can be observed only for selected clusters. The peak was observed at $T \approx 200$ K (!); the result is highly reproducible. As we know, a jump in heat capacity is a signature of a phase transition. The Al clusters are not magnetic, and therefore a magnetic

transition can be excluded. Special measurements of mobility also exclude any structural transition.

It is natural to assume that we are dealing with a transition into a superconducting state. Indeed, the calculation of T_c based on Eqns (7)–(9) leads to a value close to $T_c \approx 200$ K for Al_{45} clusters.

We note that because of the discrete nature of the electron spectrum, the lattice contribution to heat capacity is dominant at all temperatures. Nevertheless, the jump ΔC^e can be measured, because it is of an electronic nature. The experimental data in [52] (the amplitude of the observed jump and its broadness) are consistent with the described theory. The data in [52] are remarkable not only because the observed value of T_c greatly exceeds that for bulk Al but also because this is the highest observed value of the critical temperature.

The study in [52] is the first experimental observation of a high-T_c superconducting state in nanoclusters.

6.3 Diamagnetism

Pairing also leads to the appearance of orbital diamagnetism below T_c; this is analogous to the Meissner effect in usual superconductors, or to the peculiar behavior of the momenta of inertia in atomic nuclei. But the case of nanoclusters is peculiar. Indeed, we consider a magic cluster. It is characterized by a diamagnetic moment regardless of the pairing correlation; this follows just from its spherical symmetry. As a result, direct measurements of the magnetic moments do not provide a signature of the superconducting state.

Studying the special case of a cluster with two electrons (holes) in the incomplete shell (e.g., $N = 166$) can be proposed. Then the cluster should display an orbital paramagnetism at high temperatures. Indeed, because Hund's interaction in clusters is small, the linear term in the Hamiltonian dominates (the large screening, which greatly exceeds that for atoms, leads to a weak Hund's interaction). Then the transition to the superconducting state at $T = T_c$ should be accompanied by the paramagnetic–diamagnetic transition.

7. Macroscopic high-T_c superconductivity: a tunneling network

In Section 6, we discussed various manifestations of pairing in isolated clusters. Here, we consider a network that could be prepared, for example, by depositing clusters on a surface (Fig. 4). Charge transfer between clusters due to the Josephson coupling would lead to a macroscopic superconducting current at high temperatures [3, 54].

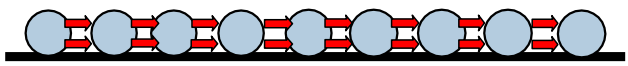

Figure 4. Cluster-based tunneling network.

7.1 Josephson coupling

As a first step, we consider two superconducting nanoclusters and the Josephson coupling between them. Based on the equation for the current,

$$\mathbf{j}(\mathbf{r}) = \frac{ie}{m}\, T \sum_n \left[\nabla_{\mathbf{r}'} - \nabla_{\mathbf{r}}\right] G_{\omega_n}(\mathbf{r}, \mathbf{r}')\big|_{\mathbf{r}=\mathbf{r}'}\,, \tag{11}$$

where G_{ω_n} is the Green's function, it can be shown that the amplitude of the current $j = j_m \sin(\varphi_1 - \varphi_2)$ is described by a relation similar to that for bulk superconductors:

$$j_m = \frac{T}{\pi e R}\, \mathrm{Im} \sum_{\omega_n} \sum_{s_1, s_2} F_1(\omega_n)\, F_2(-\omega_n)\,,$$

$$R^{-1} = 4\pi e^2 \langle |t|^2 \rangle\,. \tag{12}$$

Here, t is the tunneling matrix element and $F_i(\omega_n)$ is the Gor'kov pairing function (Eqn (1″)). For bulk superconductors (see, e.g., [55], or [56] for large nanoparticles), the summation over the states s_1, s_2 can be replaced by integration. This is not the case for the nanoclusters of interest. It can be shown [54] that the discrete nature of the spectrum and high values of T_c lead to a current density greatly exceeding that for usual bulk superconductors. It is essential that the main contribution to the sum in Eqn (12) comes from the upper shells. For bulk superconductors, $j_m \propto E_F^{-2}$, whereas for nanoclusters, $j_m \propto (\Delta E)^{-2}$. Because $E_F \gg \Delta E$, the corresponding factor increases the value of j_m. Moreover, the large degeneracy of HOS, as well as the large value of the gap parameter, is also a beneficial factor. A more detailed analysis shows that

$$\frac{j_m^{cl}}{j_m^{b}} \sim \frac{\Delta_{cl}}{\Delta_b}\, \frac{\Delta_{cl}}{\Delta E} \left(\frac{E_F}{\Delta E}\right)^2 (p_F R)^{-4}\,,$$

where Δ_{cl} and Δ_b are the cluster and bulk energy gaps, ΔE is the HOS–LUS spacing, and R is the cluster radius. For example, for the Al_{56} clusters, we obtain $j_m^{cl}/j_m^{b} \approx 3 \times 10^2$. In general, we can expect for various clusters that $j_m^{cl}/j_m^{b} \approx 10^2 - 10^3$. Therefore, the use of cluster-based tunneling networks is important not only because it would allow observing a macroscopic superconducting current at high temperatures but also because of the large gain in the amplitude of the current.

The phase of a cluster does not have a certain value; this follows from the well-known uncertainty relation between the phase and the number of particles. As a result, the phase is not defined for each of the clusters. Nevertheless, the phase difference that enters the expression for the Josephson current is defined. This fact was stressed in [56]. As usual, the phase difference is determined by the value of the transmitted current.

Macroscopic superconducting current can be transmitted by a cluster-based chain (Fig. 4). If the clusters are distributed randomly on a surface, the formation of the chain is described by the percolation theory. A similar picture was studied in [57]; the percolation chain formed by the superconducting regions embedded into a normal matrix was considered. Paper [57] was concerned with the so-called 'giant Josephson proximity effect' observed for the 'pseudogap' state of cuprates [58]. Superconducting regions form a long percolation path, transmitting the Josephson current.

For conventional superconductors, such networks were described in the interesting paper [59], which contains an analysis of a similar network. Small Pb nanoparticles were placed in an organic matrix ($C_{17}H_{33}-CO_2H$). If the initial number of nanoparticles was small, the whole system was an insulator. An increase in the number of nanoparticles resulted in tunneling between some of them and, eventually, in the formation of a percolation path. As a result, the insulator–metal transition was observed. A decrease in the temperature was accompanied by a transition to the superconducting

state: the Meissner effect was observed using SQUID magnetometry. The nanoparticles studied in [59] were relatively large, but a similar picture could be observed for the nanoclusters of interest.

The shell structure of clusters placed on a surface has to be preserved. However, shell structure has been observed only for isolated particles forming cluster beams. Cluster – surface interactions destroy this picture. The creation of a substrate (or matrix) that can keep the shell structure stable is a real challenge for material science.

7.2 Cluster crystals

A new type of crystal (crystal metals) can be created by using metallic nanoclusters as building blocks. The lattice is formed by clusters instead of the usual point-like ions. Such solids are analogous to molecular crystals. The Josephson charge transfer between neighboring superconducting clusters leads to macroscopic superconductivity. Such metals represent tunneling networks (cf. Section 7.1); in this case, the clusters form an ordered 3D lattice. Fullerides, containing C_{60} clusters, are an example of such a system. In Section 3, we mentioned the interesting paper [30], which was motivated by the discovery of superconductivity in C_{60} crystals. According to [30], the best scenario corresponds to clusters with half-filled shells.

An interesting study of Ga-based cluster metals was described in [60]. A crystal was formed by Ga_{84} clusters ($N = 252$; each Ga atom contains 3 valence electrons). A superconducting transition at $T_c \approx 7.2$ K was observed. We note that the HOS-LUS spacing for such a cluster is rather large, and there is no reason to expect a high value of T_c. Nevertheless, the value $T_c \approx 7.2$ K is noticeably higher than $T_c^b \approx 1$ K for the bulk Ga. It is useful to recall that there are two modifications of bulk Ga. One of them (ordered crystal) has the low value $T_c \approx 1$ K and the other (amorphous phase) has the large value $T_c \approx 6$ K. One might think that the clusters forming the described crystal have the amorphous structure. But the X-ray study in [60] reveals that the ions in Ga clusters are ordered. It is therefore natural to assume that the observed increase in T_c (1 K $\rightarrow$ 7.2 K) corresponds to a large T_c for Ga clusters relative to its bulk value.

8. Conclusion

Metallic nanoclusters form a new family of high-T_c superconductors. The high value of the critical temperature is caused by the shell structure of their electron spectra and the resulting high degeneracy $2(2L+1)$; the orbital momentum L for the clusters of interest is large. This high degeneracy leads to the appearance of a peak in the density of states at the Fermi level.

As is known, size quantization leads to an increase in T_c ($\delta T_c/T_c \sim 2-3$), and this effect has been observed in thin films and in granular materials [6–8, 61]. It has been explained in [62]. The phenomenon studied here is likewise concerned with size-quantized systems, but it is much larger in scale and entirely different in nature. It is caused by the shell structure and high degeneracy of orbital motion.

It is important that high T_c is not a universal property of all metallic clusters. Only selected clusters satisfy the conditions ensuring a high value of T_c (see Section 4). The manifestations of the pairing phenomenon are similar to those of pair correlation in atomic nuclei, which is a well-established concept in nuclear physics.

The theoretical treatment in [1–3] is rigorous; however, an experimental observation of the effect is a serious challenge. It requires mass spectrometry for selecting specific clusters along with special techniques for preparing cluster beams of a variable temperature. These should be combined with photoemission measurements in order to determine the electron spectrum, in particular, the magnitude of the HOS – LUS gap ΔE for $T > T_c$ and $T < T_c$. Pairing must lead to a noticeable difference in ΔE for these two temperature regions. At present, all these techniques are available, but combining them in a single experiment is a serious challenge. As regards the future progress, it lies with the construction of cluster-based tunneling networks capable of transporting macroscopic dissipationless current at high temperatures. In principle, the effect could be observed at room temperature.

For a long time, the search for new materials was mainly focused on Nb-based systems. The discovery of high-temperature cuprates [33] and the subsequent remarkable developments [34] (see also, e.g., [63]) were very important, not only because of the drastic increase in T_c. Cuprates do not contain Nb, i.e., the breakthrough came in an entirely new direction. Initially, the lesson was not very well taken, because the community worked almost exclusively with cuprates for the next 10–15 years. But in the last several years, we have been witnessing an entirely new development. Along with cuprates, scientists are now studying many novel and different superconducting systems: ruthenates, MgB_2, borocarbides, nitrides, fullerides, etc. There is also renewed interest in organic materials and heavy fermions. It is hard to recall a time when so many interesting and promising systems were being synthesized and intensively studied almost simultaneously.

The search for room-temperature superconducting material has attracted much attention [64]. Many different ideas have been put forward. They include searching for systems with negative dielectric functions [65], synthesizing crystals with specific phonon spectra [66], creating materials with a pore structure [67], and studying the superconducting state generated at interfaces in epitaxial heterostructures [68].

It follows from the analysis in this paper that nanoclusters also form a novel family, and they have promise as future room-temperature superconductors. This research, which requires the combined efforts of physicists, chemists, and material scientists, is a promising and interesting avenue.

The authors are especially grateful to J Friedel and V V Kresin for the many fruitful discussions. We also thank M Beasley, C Chu, R Dynes, L Gor'kov, M Tinkham, and S Wolf. The research by VK was supported by DARPA. The research by YO was supported by the RFBR and BNTS.

References

1. Ovchinnikov Y N, Kresin V Z *Eur. Phys. J. B* **45** 5 (2005)
2. Ovchinnikov Y N, Kresin V Z *Eur. Phys. J. B* **47** 333 (2005)
3. Kresin V Z, Ovchinnikov Y N *Phys. Rev. B* **74** 024514 (2006)
4. von Delft J, Ralph D C *Phys. Rep.* **345** 61 (2001)
5. Perenboom J, Wyder P, Meier F *Phys. Rep.* **78** 173 (1981)
6. Abeles B, in *Applied Solid State Science* Vol. 6 (Ed. R Wolfe) (New York: Academic Press, 1976) p. 1
7. Dynes R C, Garno J P, Rowell J M *Phys. Rev. Lett.* **40** 479 (1978)
8. Deutscher G *New Superconductors: From Granular to High* T_c (Hackensack, NJ: World Scientific, 2006)
9. Ralph D C, Black C T, Tinkham M *Phys. Rev. Lett.* **74** 3241 (1995); **78** 4087 (1997)
10. Black C T, Ralph D C, Tinkham M *Phys. Rev. Lett.* **76** 688 (1996)
11. Tinkham M, Hergenrother J M, Lu J G *Phys. Rev. B* **51** 12649 (1995)

12. Knight W D et al. *Phys. Rev. Lett.* **52** 2141 (1984)
13. de Heer W A *Rev. Mod. Phys.* **65** 611 (1993)
14. Brack M *Rev. Mod. Phys.* **65** 677 (1993)
15. Frauendorf S G, Guet C *Annu. Rev. Nucl. Part. Sci.* **51** 219 (2001)
16. Kresin V V, Knight W, in *Pair Correlations in Many-Fermion Systems* (Ed. V Z Kresin) (New York: Plenum Press, 1998) p. 245
17. Ring P, Schuck P *The Nuclear Many-Body Problem* (New York: Springer-Verlag, 1980)
18. Schriver K E et al. *Phys. Rev. Lett.* **64** 2539 (1990)
19. Pellarin M et al. *J. Chem. Phys.* **98** 944 (1993)
20. Ichihava T et al. *Int. J. Mass Spectrom. Ion Process.* **69** 109 (1986); Ruppel M, Rademann K *Chem. Phys. Lett.* **197** 280 (1992)
21. Lermé J et al. *Chem. Phys. Lett.* **304** 19 (1999)
22. Kresin V *J. Chem. Phys.* **128** 094706 (2008)
23. Salem L *The Molecular Orbital Theory of Conjugated Systems* (New York: W.A. Benjamin, 1966)
24. Bohr A, Mottelson B R, Pines D *Phys. Rev.* **110** 936 (1958)
25. Belyaev S T *Mat.-Fys. Medd. Danske Vid. Selsk.* **31** 131 (1959)
26. Migdal A B *Nucl. Phys.* **13** 655 (1959)
27. Labbé J, Barišić S, Friedel J *Phys. Rev. Lett.* **19** 1039 (1967)
28. Anderson P W *J. Phys. Chem. Solids* **11** 26 (1959)
29. Knight W, in *Novel Superconductivity* (Eds S A Wolf, V Z Kresin) (New York: Plenum Press, 1987) p. 47
30. Barranco M et al. *Z. Phys. D* **22** 659 (1992)
31. Boyaci H, Gedik Z, Kulik I O *J. Supercond.* **14** 133 (2001)
32. Friedel J *J. Phys. II* (France) **2** 959 (1992)
33. Bednorz J G, Müller K A *Z. Phys. B* **64** 189 (1986)
34. Wu M K et al. *Phys. Rev. Lett.* **58** 908 (1987)
35. Abrikosov A A, Gor'kov L P, Dzyaloshinski I E *Metody Kvantovoi Teorii Polya v Statisticheskoi Fizike* (Methods of Quantum Field Theory in Statistical Physics) 3rd ed. (Moscow: Dobrosvet, 2006) [Translated into English: 1st Rev. English ed. (New York: Dover Publ., 1975)]
36. Gor'kov L P *Zh. Eksp. Teor. Fiz.* **34** 735 (1958) [*Sov. Phys. JETP* **7** 505 (1958)]
37. Scalapino D J, in *Superconductivity* Vol. 1 (Ed. R Parks) (New York: M. Dekker, 1969) p. 449
38. Grimvall G *The Electron-Phonon Interaction in Metals* (Amsterdam: North-Holland, 1981)
39. Karakozov A E, Maksimov E G, Mashkov S A *Zh. Eksp. Teor. Fiz.* **68** 1937 (1975) [*Sov. Phys. JETP* **41** 971 (1975)]
40. Eliashberg G M *Zh. Eksp. Teor. Fiz.* **39** 1437 (1960) [*Sov. Phys. JETP* **12** 1000 (1961)]
41. Heiselberg H *Phys. Rev. A* **63** 043606 (2001)
42. Yannouleas C, Broglia R A *Ann. Phys.* (New York) **217** 105 (1992)
43. Cohen M, in *Superconductivity* Vol. 1 (Ed. R Parks) (New York: M. Dekker, 1969) p. 615
44. McMillan W L *Phys. Rev.* **167** 331 (1968)
45. Owen C S, Scalapino D J *Physica* **55** 691 (1971)
46. Kresin V Z, Gutfreund H, Little W A *Solid State Commun.* **51** 339 (1984)
47. Kresin V Z *Phys. Lett. A* **122** 434 (1987)
48. Ekardt W *Phys. Rev. B* **29** 1558 (1984)
49. Moro R et al. *Science* **300** 1265 (2003)
50. Wrigge G, Astruk Hoffmann M, v. Issendorff B *Phys. Rev. A* **65** 063201 (2002); Wrigge G et al. *Eur. Phys. J. D* **24** 23 (2003)
51. von Issendorff B, Cheshnovsky O *Annu. Rev. Phys. Chem.* **56** 549 (2005)
52. Cao B et al., arXiv:0804.0824
53. Breaux G A et al. *Phys. Rev. Lett.* **94** 173401 (2005)
54. Kresin V, Ovchinnikov Y "Cluster-based tunneling network", Preprint (Berkeley, CA: Lawrence Berkeley Laboratory, Univ. of California)
55. Kulik I, Yanson I *The Josephson Effect in Superconductive Tunneling Structures* (Jerusalem: Israel Program for Scientific Translations 1972)
56. Gobert D, Schollwock U, von Delft J *Eur. Phys. J. B* **38** 501 (2004)
57. Kresin V, Ovchinnikov Y, Wolf S *Appl. Phys. Lett.* **83** 722 (2003)
58. Bozovic I et al. *Phys. Rev. Lett.* **93** 167002 (2004)
59. Weitz I et al. *J. Phys. Chem.* **104** 4288 (2004)
60. Hagel J et al. *J. Low Temp. Phys.* **129** 133 (2002)
61. Strongin M, Kammerer O, Parkin A *Phys. Rev. Lett.* **14** 949 (1965)
62. Parmenter R *Phys. Rev.* **166** 392 (1968)
63. Wolf S A, Kresin V Z (Eds) *Novel Superconductivity* (New York: Plenum Press, 1988)
64. Ginzburg V L *Usp. Fiz. Nauk* **175** 187 (2005) [*Phys. Usp.* **48** 173 (2005)]
65. Chu C et al., cond-mat/0511166
66. Pickett W *J. Supercond.* **19** 291 (2006)
67. Zakhidov A et al. *Science* **282** 897 (1998)
68. Reyren N et al. *Science* **317** 1196 (2007)